Polymer Journal, Vol. 24, No. 11, pp 1271—1280 (1992)

Crystallization of Block Copolymers II. Morphological Study of Poly(ethylene glycol)–Poly(ε-caprolactone) Block Copolymers†

Shuichi NOJIMA,* Mitsugu ONO, and Tamaichi ASHIDA

Department of Biotechnology, School of Engineering, Nagoya University, Nagoya 464-01, Japan

(Received May 14, 1992)

ABSTRACT: Block copolymers consisting of poly(ethylene glycol) (PEG) and poly(ε-caprolactone) (PCL) were synthesized by adding ε-caprolactone to the PEG ends, and the morphology and melting behavior of these copolymers were investigated by small-angle X-ray scattering (SAXS), wide-angle X-ray diffraction (WAXD), and differential scanning calorimetry (DSC). A binary blend of PEG and PCL oligomers was also prepared to compare the morphology with that of the copolymers. The long spacing L, an alternate period of the lamella and amorphous layer, evaluated from the angular position of the SAXS maximum dramatically decreased by adding a short PCL block to the PEG ends, and then increased linearly with connected PCL block length. The melting temperature T_m showed maximum depression of *ca.* 20°C for the copolymer with an equal proportion of the PEG and PCL blocks. The WAXD results revealed that the crystals of the PEG and PCL blocks independently existed and there was no diffraction from an eutectic crystal composed of the two blocks. In the PEG/PCL blend, L and T_m did not change with changing the PCL fraction and exactly corresponded to those of the constituent homopolymers. These facts suggest that the covalent bond between the PEG and PCL blocks restricts the formation of the favorable crystalline morphology which appears in the PEG/PCL blend, and eventually a characteristic morphology is formed in these copolymer systems.

KEY WORDS Crystalline-Crystalline Block Copolymer / Morphology / Small-Angle X-ray Scattering / Wide-Angle X-ray Diffraction / Differential Scanning Calorimetry /

The crystallization of synthetic homopolymers has been extensively studied from morphological and kinetic viewpoints.[1] In the homopolymer crystallization, a perfect crystal is seldom or never obtained and an alternate structure consisting of the lamellae and amorphous layers usually appears, the details of which are mainly determined by the kinetic factors during crystallization. In the case of crystalline-amorphous diblock copolymers, the amorphous block which can not inherently crystallize intervenes during crystallization. The amorphous block is, as a result, forced to stay on the lamellar surface and thermodynamically restricts the fold number of the crystalline block when the copolymer is gradually cast from the solution.[2,3] When such a copolymer is quenched from the melt, it may have a microphase structure and this will give a significant influence on the following crystallization of the constituent block.[4] There are several studies on the crystalline morphology of diblock copolymers.[4-13] We recently investigated the morphology and the process

* To whom correspondence should be addressed.

† For Part I, see ref 4.

of the morphology formation of poly(ε-caprolactone)-*block*-polybutadiene[4] and found that the crystallization of the PCL block was significantly affected by the preceding microphase separation to yield a considerable difference in the morphology formation between block copolymers and polymer blends.[14-17]

In the case of crystalline–crystalline block copolymers, two kinds of crystallization may work simultaneously as well as the microphase separation, and eventually a complicated morphology may be formed. The morphology of such copolymers was previously investigated by the dilatometric and diffractometric techniques.[18,19] It is, however, necessary to quantitatively discuss the crystalline morphology of such copolymers by taking account of the covalent bond between chemically different blocks.

In the present study, we investigate the morphology of block copolymers with poly(ethylene glycol) (PEG) and poly(ε-caprolactone) (PCL), where both chains are crystallizable. A recent development of non-catalystic polymerization made it possible to synthesize such copolymers with various block lengths.[20] It is, therefore, possible to quantitatively discuss the change of the crystalline morphology by systematically changing the block length of the copolymer. The electron densities of the amorphous PCL and PEG chains are, however, very close (341.6 and 354.3 e nm^{-3} for the amorphous PCL[21] and PEG,[22] respectively, at 80°C), so that it is not appropriate to study the homogeneous state and microphase structures of these copolymers by X-ray scattering. The crystalline morphology is conveniently investigated by small-angle X-ray scattering (SAXS) because the electron density difference between the PCL (or PEG) crystal and amorphous PCL (or PEG) is adequately large. (392.9 and 403.2 e nm^{-3} for perfect crystals of PCL[23] and PEG,[24] respectively) The morphology of the copolymers crystallized at various temperatures was investigated by SAXS, and the melting behavior was observed by differential scanning calorimetry (DSC). The crystallinity of the PEG and PCL blocks was also evaluated by wide-angle X-ray diffraction (WAXD). A binary compatible blend of PEG and PCL oligomers was also prepared to compare the morphology with that of the copolymers.

EXPERIMENTAL

Materials and Sample Preparation

The block copolymers used in this study were synthesized by adding ε-caprolactone to poly(ethylene glycol) (PEG) of low molecular weight without any catalyst followed by the method of Cerrai *et al.*[20] The PEG (PEG1, $M_w = 6{,}200$), recrystallized from a mixture of diethyl ether and tetrahydrofuran, was first dissolved in distilled ε-caprolactone monomer and then block copolymer was polymerized at *ca.* 200°C for 22—76 h under vacuum. The reaction time was adjusted so as to obtain copolymers with various PCL block lengths. It was shown by Cerrai *et al.* employing ^{1}H nuclear magnetic resonance (NMR) and infra-red spectroscopy (IR) that the PCL homopolymer is not yielded through the reaction and that the product is an A–B–A type block copolymer of a narrow molecular weight distribution with the PEG chain being middle.[18] The product was treated with diethyl ether to remove the unreacted PEG. The result of gel permeation chromatography (GPC) showed that there was no PEG prepolymer remaining after purification, and the molecular weight of the copolymer steadily increased with increasing the reaction time. The molecular characterization of the copolymers together with the PEG and PCL homopolymers, which was performed by GPC and elementary analysis, is shown in Table I.

A binary blend of PEG and PCL was also used to compare the morphology and the melting behavior with those of the copolymers, where PEG2 ($M_w = 2{,}560$) was used instead

Table I. Characterization of the polymers

Notation	Polymer	Source	M_w of PEG	Total M_w[d]	M_w/M_n[d]	PCL : PEG : PCL[e]
A1	PCL-*b*-PEG-*b*-PCL	a	6200	6700	1.05	4 : 92 : 4
A2	PCL-*b*-PEG-*b*-PCL	a	6200	10100	1.06	19 : 62 : 19
A3	PCL-*b*-PEG-*b*-PCL	a	6200	14200	1.10	28 : 44 : 28
A4	PCL-*b*-PEG-*b*-PCL	a	6200	29900	1.15	39 : 22 : 39
A5	PCL-*b*-PEG-*b*-PCL	a	6200	48600	1.27	43 : 14 : 43
PEG1	PEG	b		6200	1.05	
PEG2	PEG	c		2560	1.08	
PCL1	PCL	a		8200	1.59	

[a] Synthesized in our laboratory.
[b] Obtained from Kishida Chemicals Inc.
[c] Obtained from American Polymer Standards Corp.
[d] Determined by GPC.
[e] Determined by elementary analysis assuming an equal molecular weight for both PCL blocks.

of PEG1 to obtain the compatibility with PCL1 at temperatures above the melting point of PEG and PCL. The solvent-casting method was employed to prepare blends with various compositions. That is, PEG2 and PCL1 were dissolved in a common solvent, toluene, the solution was cast on a glass plate, and the solvent was evaporated under vacuum at 80°C for more than 40 h.

Differential Scanning Calorimetry (DSC) Measurement[25]

A MAC Science Model 3100 DSC was used to determine the melting temperature of PEG and PCL. The sample, first annealed at 80°C for 1 h, was crystallized by quenching to the crystallization temperature T_c, followed by heating at a rate of 5 deg min^{-1}. The quench process was completely finished before the copolymer started to crystallize. Exothermic heat flow during crystallization was also monitored to ensure the end of crystallization. Melting temperature was evaluated from the peak position of the major endothermic curve.

It was impossible to evaluate the crystallinity of individual PCL and PEG blocks from the heat of fusion, because the melting temperature of PEG and PCL falls on a same temperature range.

Small-Angle X-ray Scattering (SAXS) Measurement[26]

SAXS measurement was performed with a pin-hole collimation system and a one-dimensional position sensitive proportional counter (PSPC) made by Rigaku Co. Nickel-filtered Cu-K_α radiation ($\lambda = 0.1542$ nm) supplied from a rotating anode X-ray generator (Rigaku RU-300) operated at 50 kV and 80 mA was used. The distance between the sample and PSPC was about 400 mm. After SAXS intensity was corrected for the linearity and sensitivity of the PSPC, background scattering, and the Lorentz factor, relative scattered intensity was obtained as a function of wave number s ($=(2/\lambda)\sin\theta$, 2θ: scattering angle).

SAXS intensity was measured after the sample was quenched from the melt and completely crystallized in the sample cell of the SAXS apparatus for about 1 h at each temperature (T_c), which was adequately controlled by circulating water with a constant temperature. The time necessary for each measurement was 2000 s, during which the sample was kept at each T_c within the fluctuation of 0.1°C.

Wide-Angle X-ray Diffraction (WAXD) Measurement

WAXD measurement was performed by

using a conventional equipment with the X-ray film as a detector. The sample was 0.2 mm in thickness for all measurements and the distance between the sample and the film was 65 mm. The WAXD pattern was circularly averaged and relative intensity was evaluated as a function of the diffraction angle 2θ after the background correction. The diffraction from the copolymer was decomposed into the diffractions from the PEG and PCL crystals, and the crystallinity of the PEG and PCL blocks was evaluated assuming that the WAXD pattern for the copolymer is a linear combination of those for PEG and PCL crystals.

RESULTS

Small-Angle X-ray Scattering (SAXS) Curves

Figure 1 shows the Lorentz-corrected SAXS curves for PEG1 and various copolymers crystallized at 35°C. The SAXS curves for PEG1, A1, and A2 have a set of intensity maxima at finite s, which disappear at temperatures above the melting point of the PCL and PEG crystals. The angular position of these intensity maxima strictly corresponds to the higher-order diffractions of the first peak. The SAXS curves for A3 and A5, on the other hand, have a broad intensity maximum and are reminiscent of that for the PCL homopolymer (Figure 2). The copolymers at the melt did not show any sharp diffraction based on the microphase structure of the block copolymer nor the diffuse scattering maximum due to the correlation hole effect of homogeneous block copolymers, probably because of a close proximity of the electron density between the PCL and PEG chains at the molten state.

Figure 2 shows the Lorentz-corrected SAXS curves for PEG2, PCL1, and various PEG2/PCL1 blends indicated. The SAXS curve for the blends is obviously a superposition of those for the homopolymers; the angular positions of the maxima agree well with those for PEG2 and in addition there is a peak or shoulder

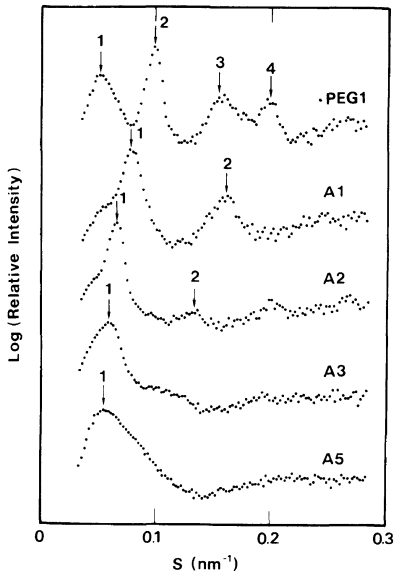

Figure 1. Lorentz-corrected SAXS intensities, scattered from PEG1 and various block copolymers crystallized at 35°C, are plotted against s ($=2\sin\theta/\lambda$). The plots for PEG1, A1, A2, and A3 shift upward successively for legibility. The order of each scattering maximum is indicated by the number.

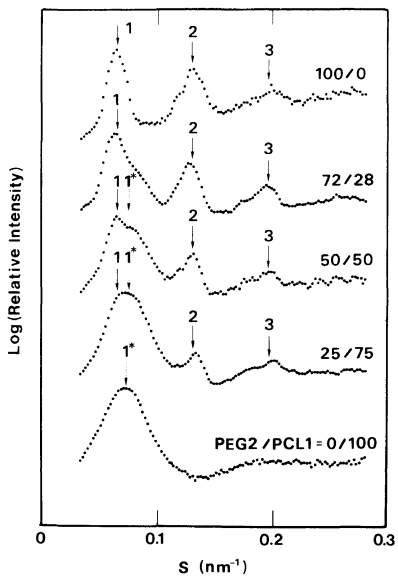

Figure 2. Lorentz-corrected SAXS intensities, scattered from various PEG2/PCL1 blends crystallized at 35°C, are plotted against s. The order of the scattering maximum for PEG2 is indicated by the number and that for PCL1 is indicated by the number with asterisk.

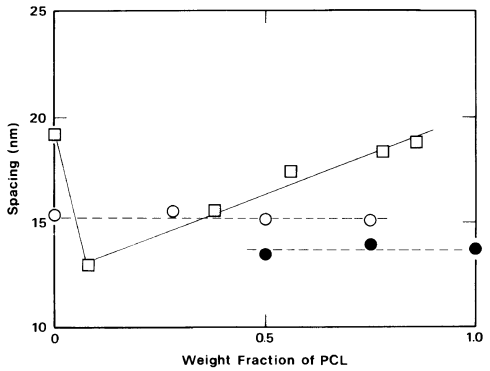

Figure 3. The long spacing, evaluated from the angular position of the SAXS maximum, is plotted against the weight fraction of PCL in the system. The square represents the results of the copolymers with PEG1 being the middle block. The SAXS curve scattered from the binary blends was the superposition of those from PEG2 and PCL1 and therefore two spacings which corresponded to PEG2 (○) and PCL1 (●) could be evaluated.

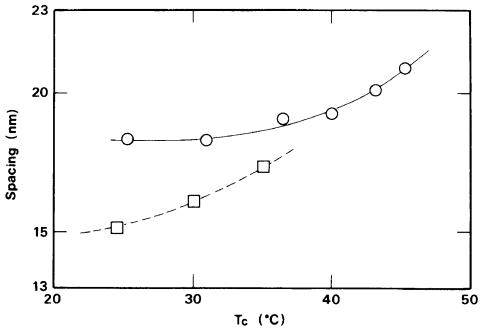

Figure 4. The long spacing, evaluated from the angular position of the SAXS maximum for A3 (□) and PEG1 (○), is plotted against crystallization temperature T_c.

arising from PCL1 in the vicinity of the first peak position. This suggests that the morphology of the PEG2/PCL1 blend is a mosaic structure independently consisting of the PEG and PCL domains in which each polymer crystallizes without any mutual influence in the form of the alternate structure of the lamellae and amorphous layers (see Figure 10).

The long spacing L, an alternate distance of the lamella and amorphous layer, can be evaluated from the angular position of the SAXS maxima of Figures 1 and 2, and is plotted in Figure 3 against the PCL fraction. L of PEG1 is about 19 nm, which is dramatically depressed by the addition of the short PCL block to the PEG ends. This sudden decrease of L or lamellar thickness has been reported when the ends were replaced with a bulky group such as phenyl group,[27,28] which arises from the change of the chain-folding nature in the lamellar crystal. That is, the specific interaction between PEG ends at the melt vanishes by replacing the hydroxyl group with a bulky group, which brings about the increase of the chain-folding number and/or the irregular lamellar surface after crystallization to result in a large reduction of L.[27] It is also reported that the size of the bulky group does not significantly affect the resulting lamellar thickness.[28] A further addition of ε-caprolactone makes L gradually larger as shown in Figure 3, indicating that the amorphous layer thickness increases. In this amorphous layer, the PCL block may crystallize with increasing its chain length, and eventually only the PCL chain crystallizes with the PEG chain being amorphous when the PCL block is dominant in the copolymer. Two values of L could be evaluated from the SAXS curve for the binary blends, each comparable to those for PEG2 and PCL1. This also strongly confirms that the PEG and PCL polymers do not influence each other during crystallization to form the individual domains. The crystalline morphology of the copolymer is, on the other hand, difficult to presume only from the SAXS results, though the major component in the copolymer seems to control the final morphology.

The crystallization temperature (T_c) dependence of L is shown in Figure 4 for PEG1 and A3. Because the melting temperature of the copolymers is significantly depressed (Figure 5), the T_c range of A3 is limited in a narrow temperature range. As can be seen in Figure 4, L increases with T_c for both PEG1 and A3. This is an usual observation for the

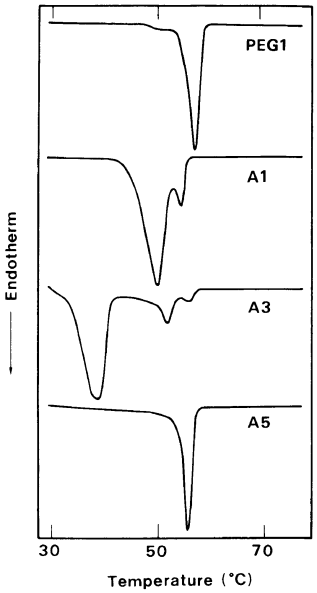

Figure 5. DSC thermograms for PEG1, A1, A3, and A5 crystallized at 35°C for 1 h. The heating rate was 5°C min^{-1}. The melting temperature T_m was the temperature at which the endothermic peak was maximum.

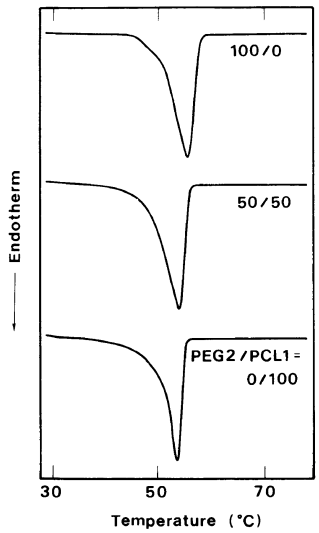

Figure 6. DSC thermograms for PEG2, PCL1, and their 50/50 binary blend.

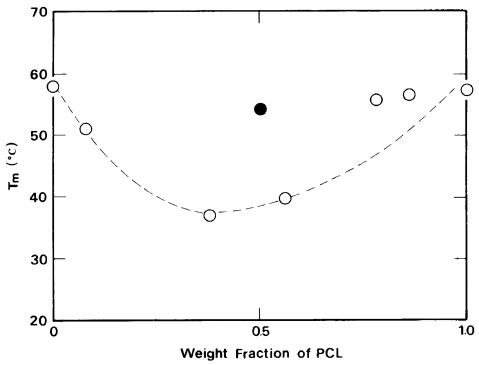

Figure 7. Major melting temperature T_m is plotted against the weight fraction of PCL in the copolymer. The closed circle represents the results with the PEG2/PCL1 blend.

homopolymer crystallization and the distance between T_c and the equilibrium melting temperature T_m^0, $T_m^0 - T_c$, is used instead of T_c as a measure to decide L for a homolog with different T_m^0. Copolymers with different molecular weights or different block ratios may have different T_m^0. This variation of T_m^0 among copolymers, therefore, may be partly responsible for the variation of L shown in Figure 3, because $T_m^0 - T_c$ may be rather different for individual copolymers crystallized at a same T_c. The change of L with T_c (or $T_m^0 - T_c$) shown in Figure 4 is, however, not adequate to completely explain the large change of L with changing the PCL fraction shown in Figure 3. This large change of L will be accompanied by the morphological change attributable to the difference in the block ratio of the copolymers.

Differential Scanning Calorimetry (DSC) Measurement

Figure 5 shows the DSC curves for PEG1 and various copolymers crystallized at 35°C and Figure 6 shows those for PEG2, PCL1, and their 50/50 binary blend. The heating rate was 5°C min^{-1} and the heating rate dependence could not be detected. PEG1 (and also PEG2) and PCL1 have a single endothermic peak at temperatures around 58°C. The melting temperature of the copolymers depresses significantly when it is plotted in Figure 7 against the PCL fraction in the copolymer. Figure 7 shows the maximum

depression of *ca.* 20°C and is nearly symmetrical against the PCL fraction. The melting temperature of the binary blend, on the other hand, is intermediate between two homopolymers as shown by the closed circle in Figure 7. Cerrai *et al.* observed similar melting point depression of the PEG crystal for the copolymers they synthesized,[20] where they used a shorter PEG prepolymer whose T_m was 41°C. They qualitatively explained that in the process of the morphology formation, the PCL block crystallized first ($T_m = 56$—58°C) and this led to freezing of the whole morphology, and eventually imperfectness of the PEG lamellar crystal. In the present study, both PEG and PCL crystals had a comparable T_m and a large melting point depression for both crystals could be observed. That is, the crystallization of each block extremely influence each other to yield imperfect PEG and PCL crystals simultaneously. This also suggests a large difference in the morphology after crystallization between the binary blend and block copolymers.

The melting point depression of the crystalline polymer in a compatible blend arises from the kinetic and thermodynamic effects. The kinetic effect functions during crystallization and brings about the variation of the lamellar thickness which is theoretically related to T_m through the equation,[29]

$$T_m = T_m^0\left(1 - \frac{2v_e}{\Delta H_f L}\right) \quad (1)$$

where v_e is the free energy of chain folding at the surface of the lamella and ΔH_f is the heat of fusion of the lamella. Therefore, the reduction of the lamellar thickness leads to the melting point depression. The covalent bond between different blocks is, however, expected to be a dominant origin to reduce L in the present system. The thermodynamic effect works by blending other components and can be estimated on the basis of the Flory–Huggins–Scott theory[30,31] for compatible blend systems. Though this equation should be modified for the present copolymer systems, the melting point will be strongly dependent on the interaction parameter between two blocks as well as the volume fraction of each block.[32] The melting point depression of the present copolymer systems arises from the sum of the above two effects and will be complicated because each lamella is formed simultaneously with mutual influence during crystallization. No detectable melting point depression for the PEG/PCL blends suggests that both effects do not work effectively in the blend.

Wide-Angle X-ray Diffraction (WAXD) Measurement

It was impossible in the present study to evaluate the crystallinity of the PEG and PCL chains from the heat of fusion because of a close proximity of the melting temperature of the crystals. Wide-angle X-ray diffraction (WAXD) is an alternate method to evaluate the crystallinity of these chains, because the crystal structure and therefore the characteristic diffractions are quite different between PEG and PCL crystals.

Figure 8 shows the WAXD patterns from the PEG and PCL crystals and various copolymers indicated. The major diffraction peaks of PEG and PCL could be successfully indexed. The WAXD pattern from A2 and A3 is the superposition of those of the PEG and PCL crystals, while A1, A4, and A5 substantially show the same diffraction with the major component in the copolymer. (*i.e.*, PEG for A1 and PCL for A4 and A5) Figure 8 means that there is no eutectic crystal or mixed crystal consisting of both the PEG and PCL chains, and the PEG and PCL crystals are independently existing in the system.

The WAXD pattern from A2 and A3 is composed of the contributions from the PEG and PCL crystals and if we assume that there is no interaction between the diffractions from both the crystals, the WAXD intensity $I(\theta)$ for A2 and A3 is expressed as,

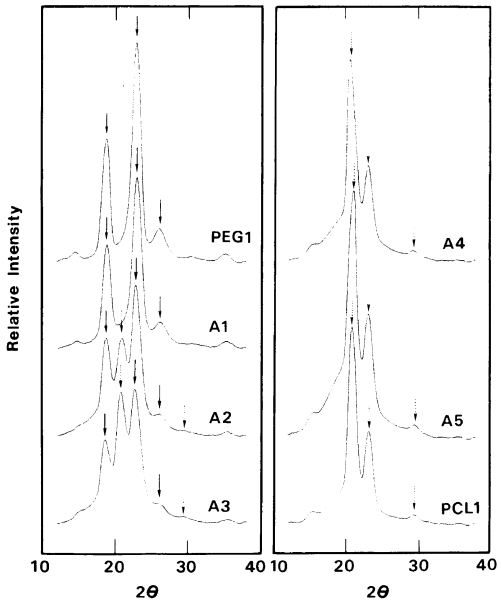

Figure 8. WAXD patterns from PEG1, PCL1, and various copolymers are plotted against diffraction angle 2θ. The WAXD patterns from A2 and A3 are the superposition of those of PEG1 and PCL1. The solid arrows represent the diffractions from PEG1 and the dotted arrows from PCL1.

$$I(\theta) = x_{PCL} I_{PCL}(\theta) + x_{PEG} I_{PEG}(\theta) \qquad (2)$$

where x_{PCL} and x_{PEG} are the actual crystallinity of the PCL and PEG chains in the copolymer, respectively. $I_{PCL}(\theta)$ and $I_{PEG}(\theta)$ are diffraction intensities from the PCL and PEG homopolymers with 100% crystallinity and can be derived from Figure 8 with the DSC crystallinity. Using eq 2 it is possible to evaluate x_{PCL} and x_{PEG} by dividing the diffraction curve from A2 and A3 into the contributions from the PEG and PCL homopolymers by a least-squares method. The crystallinity of the PEG and PCL chains thus evaluated is plotted in Figure 9, together with DSC results, against the PCL fraction in the system. The agreement is satisfactory between the results derived from the two independent methods. The crystallinity of the PEG and PCL chains decreases with decreasing each block fraction and falls to zero when the corresponding block fraction is less

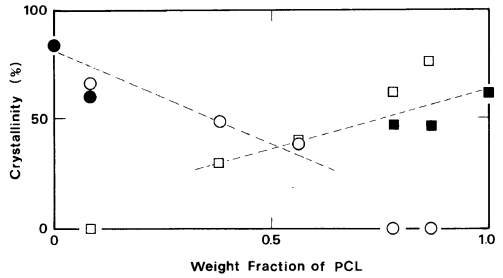

Figure 9. Crystallinity of the PEG (○, ●) and PCL (□, ■) chains is plotted against the weight fraction of PCL in the copolymer. The open symbols (○, □) were evaluated from WAXD results and the closed symbols (●, ■) from DSC results.

than 25% in the system. The copolymers with the PCL fraction around 50% have both the crystals, indicating that the morphology is formed by the competition of the PEG and PCL crystallizations. In the binary blend, on the other hand, PEG and PCL crystallize independently even if the fraction of the minor component is less than 25%, as shown in Figure 3. This point is a significant difference between the block copolymer and the polymer blend and brings about a significant difference in the crystalline morphology between both the systems.

DISCUSSION

The morphology and melting behavior of block copolymers consisting of two different crystalline chains, poly(ethylene glycol) (PEG) and poly(ε-caprolactone) (PCL), were investigated in the present study by small-angle X-ray scattering (SAXS), wide-angle X-ray diffraction (WAXD), and differential scanning calorimetry (DSC). A binary blend of PEG and PCL oligomers was also prepared to compare the morphology with that of the copolymers. The SAXS measurement showed a dramatic decrease of the long spacing by adding a short PCL block to the PEG ends, and then increased linearly with PCL block length. The WAXD measurement demonstrated a coexistence of the PEG and PCL crystals for the copolymers

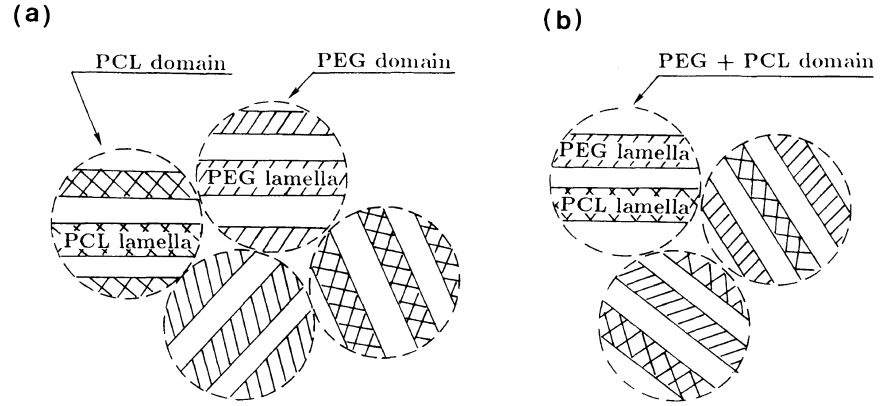

Figure 10. Schematic illustration of the morphology formed in the PEG/PCL blend (a) and the PEG-PCL block copolymer (b). In the blend, PEG and PCL are phase-separated into domains in which each homopolymer crystallizes in a lamellar texture. In the copolymer PEG and PCL blocks crystallize in a same domain with mutual influence during crystallization.

with a nearly equal proportion of the PEG and PCL blocks, while only one crystal of the major component for other copolymers. There was no eutectic crystal detected composed of the PEG and PCL blocks. The DSC measurement showed that the melting temperature took a minimum, which was about 20°C lower than the corresponding homopolymers. The SAXS curve for the PEG/PCL blend was a superposition of those for the PEG and PCL homopolymers and two spacings could be evaluated which strictly corresponded to those of the homopolymers. The melting temperature of the PEG and PCL chains in the blend did not change with change in the PCL fraction and was comparable to those of the corresponding homopolymers.

The morphology for the PEG/PCL blend is not difficult to image from the combined results of SAXS and DSC, where the long spacing and the melting point are not influenced by the existence of the other component. This indicates that even if the PEG and PCL oligomers are compatible at the melt, they segregate each other by the crystallization and make individual domains in which each homopolymer forms the alternate structure of the lamellae and amorphous layers. It is shown in Figure 10(a) and widely observed in compatible crystalline/crystalline blends such as high density polyethylene/low density polyethylene[33] and poly(ethylene oxide)/poly-(3-hydroxy butyrate)[34] systems. That is, the formation of a lamella does not influence that of another and as a result no depression of the melting temperature of each crystal nor reduction of the long spacing occurs in these blend systems.[35] In the case of the present crystalline–crystalline block copolymer systems, on the other hand, the different chains are connected by the covalent bond. It is, therefore, impossible to make a large-scale segregation after crystallization and constituent chains exist within a domain. When one component (PEG or PCL) is dominant in the copolymer, it crystallizes and the minor component, rejected from the crystal, is accommodated in the amorphous layer between the lamellae. The morphology will be similar to that observed in a compatible crystalline/amorphous blend. When the two components are of a comparable fraction, they crystallize simultaneously and each crystal coexists within a domain as illustrated in Figure 10(b). The two crystals influence each other during crystallization resulting in the large

reduction of the lamellar thickness (or long spacing) and the imperfectness of the crystals (or melting temperature depression) as measured by SAXS and DSC. Figure 10(b) also successively explains the WAXD pattern which is a superposition of the diffractions of the PEG and PCL crystals, because each crystal certainly exists in the crystalline morphology and there is no mixed crystal composed of the PEG and PCL chains. The characteristics of the morphology of such systems have hitherto been pointed out qualitatively from dilatometric results[18,19] and from DSC results.[20] But, the present results with the combination of SAXS, DSC, and WAXD comprehensively support the morphological differences shown in Figure 10.

Schematic picture illustrated in Figure 10(b) seems to explain all the experimental results in the present study and is conceivable from the covalent bond between two different blocks. The validity of the morphology presented in Figure 10, however, should be confirmed by the microscopic technique and the morphology should be quantitatively evaluated as a function of the molecular characteristics of the copolymers.

Acknowledgment. We thank the staff of the Workshop for Experimentation and Practice, School of Engineering, Nagoya University, for making the vacuum line to synthesize the samples used in the present study.

REFERENCES AND NOTES

1. B. Wunderlich, "Macromolecular Physics," Vols. 1—3, Academic Press, New York, N. Y., 1973.
2. E. A. DiMarzio, C. M. Guttman, and J. D. Hoffman, *Macromolecules*, **13**, 1194 (1980).
3. M. D. Whitmore and J. Noolandi, *Macromolecules*, **21**, 1482 (1988).
4. S. Nojima, K. Kato, S. Yamamoto, and T. Ashida, *Macromolecules*, **25**, 2237 (1992).
5. P. C. Ashman and C. Booth, *Polymer*, **16**, 889 (1975).
6. P. C. Ashman, C. Booth, D. R. Cooper, and C. Price, *Polymer*, **16**, 897 (1975).
7. M. Gervais and B. Gallot, *Polymer*, **22**, 1129 (1981).
8. I. S. Zemel, J. P. Corrigan, and A. E. Woodward, *J. Polym. Sci., B*, **27**, 2479 (1989).
9. R. E. Cohen, P. L. Cheng, K. Douzinas, P. Kofinas, and C. V. Berney, *Macromolecules*, **23**, 324 (1990).
10. C. A. Veith, R. E. Cohen, and A. S. Argon, *Polymer*, **32**, 1545 (1991).
11. K. C. Douzinas, R. E. Cohen, and A. F. Halasa, *Macromolecules*, **24**, 4457 (1991).
12. S. Ishikawa, K. Ishizu, and T. Fukutomi, *Polym. Commun.*, **32**, 374 (1991).
13. R. Unger, D. Beyer, and E. Donth, *Polymer*, **32**, 3305 (1991).
14. S. Nojima, H. Tsutsui, M. Urushihara, W. Kosaka, N. Kato, and T. Ashida, *Polym. J.*, **18**, 451 (1986).
15. S. Nojima, Y. Terashima, and T. Ashida, *Polymer*, **27**, 1007 (1986).
16. S. Nojima, K. Satoh, and T. Ashida, *Macromolecules*, **24**, 942 (1991).
17. S. Nojima, K. Kato, M. Ono, and T. Ashida, *Macromolecules*, **25**, 1922 (1992).
18. R. Perret and A. Skoulios, *Makromol. Chem.*, **162**, 147 (1972).
19. R. Perret and A. Skoulios, *Makromol. Chem.*, **162**, 163 (1972).
20. P. Cerrai, M. Tricoli, F. Andruzzi, M. Paci, and M. Paci, *Polymer*, **30**, 338 (1989).
21. V. Crescenzi, G. Manzini, G. Calzolari, and C. Borri, *Eur. Polym. J.*, **8**, 449 (1972).
22. A. Sikora, *Collect. Czechoslovak Chem. Commun.*, **50**, 2146 (1985).
23. Y. Chatani, Y. Okita, H. Tadokoro, and Y. Yamashita, *Polym. J.*, **1**, 555 (1970).
24. Y. Takahashi and H. Tadokoro, *Macromolecules*, **6**, 672 (1973).
25. S. Nojima, D. Wang, and T. Ashida, *Polym. J.*, **23**, 1473 (1991).
26. Z. Zheng, S. Nojima, T. Yamane, and T. Ashida, *Macromolecules*, **22**, 4362 (1989).
27. N. Okui, S. Shimada, and T. Kawai, *Kobunshi Ronbunshu*, **31**, 215 (1974).
28. C. Booth, R. C. Domszy, and Y. K. Leung, *Makromol. Chem.*, **180**, 2765 (1979).
29. J. I. Lauritzen and J. D. Hoffman, *J. Appl. Phys.*, **44**, 4340 (1973).
30. P. J. Flory, "Principles of Polymer Chemistry," Cornell Univ. Press, Ithaca, New York, N.Y., 1953.
31. R. L. Scott, *J. Chem. Phys.*, **17**, 279 (1949).
32. T. Nishi and T. T. Wang, *Macromolecules*, **8**, 909 (1975).
33. S. R. Hu, T. Kyu, and R. S. Stein, *J. Polym. Sci., B*, **25**, 71 (1987).
34. M. Avella, E. Martuscelli, and P. Preco, *Polymer*, **32**, 1647 (1991).
35. The domain boundary illustrated in Figure 10 is rather ambiguous. The domain should be defined as the region in which the SAXS intensity from each lamella correlates each other.